The rotational and hyperfine spectrum and structure of H2CO–HF2

F. A. Baiocchi and W. Klemperer

Citation: The Journal of Chemical Physics **78**, 3509 (1983); doi: 10.1063/1.445174
View online: http://dx.doi.org/10.1063/1.445174
View Table of Contents: http://scitation.aip.org/content/aip/journal/jcp/78/6?ver=pdfcov
Published by the AIP Publishing

The rotational and hyperfine spectrum and structure of H_2CO–HF[a)]

F. A. Baiocchi and W. Klemperer

Department of Chemistry, Harvard University, Cambridge, Massachusetts 02139
(Received 30 August 1982; accepted 8 November 1982)

The rotational spectrum of the hydrogen bonded complex formed between hydrogen fluoride and formaldehyde has been obtained from 3 to 55 000 MHz using molecular beam electric resonance spectroscopy. The molecule is found to be a prolate slightly asymmetric rotor with $\kappa = -0.98$ and an inertial defect of $\Delta = 0.62$ amu Å^2. The rotational constants determine that the average geometry of the three heavy atoms is bent with an O–F distance of 2.66 Å and a C–O–F angle of 109.5°. The large value of μ_a shows that HF is hydrogen bonded to the oxygen. The average orientation of the HF axis with respect to the inertial axes is obtained from the two components (S_a and S_b) of the direct nuclear spin–spin hyperfine coupling tensor. Both the hyperfine data and the value of μ_b indicate a nonlinear hydrogen bond in this species. Finally, the observation of hyperfine splittings in the spectrum attributable to the presence of the triplet spin state of formaldehyde provides experimental information regarding the tunneling of the formaldehyde protons. The spectra is consistent with a rigid planar structure. Some of the spectroscopic and average structural constants are summarized: $A - \Delta_K = 50\,543.205(23)$ MHz; $B = 4832.232(33)$ MHz; $C = 4386.621(33)$ MHz; $\mu_a = 3.7535(2)$ D; $\mu_b = 1.399(1)$ D; $S_a^{HF} = 93.6(8)$ kHz; $S_b^{HF} = -31.7(11)$ kHz; $r_{O\text{-}H} = 1.794$ Å; $r_{O\text{-}F} = 2.659$ Å; $\angle C = O\cdots F = 109.5°$; $\angle C = O\cdots H = 115°$.

INTRODUCTION

The already rich variety of hydrogen bonded structures that are known from crystallography, has been greatly enhanced by rotational spectroscopy of gas phase hydrogen bonded complexes. The contributions of Bill Flygare to this field are of singular noteworthiness. In this paper we pursue the study of a system closely related to some recent work of Flygare.

Weakly bound molecular complexes of the form $R_1R_2C = O \cdots HA$, with HA an acid, constitute an important class of hydrogen bonded species, examples of which are found in many areas of chemical interest. For example, their existence in acidic solutions of aldehydes and ketones has long been postulated to explain the acid catalyzed reaction of nucleophiles with the carbonyl group.[1] There has been great interest in characterizing their structure and dynamics, as is evidenced by the large number of experimental studies of such complexes. The structural determinations have mainly consisted of x-ray and neutron diffraction studies on crystalline forms of the complexes.[2] The internal dynamics of complexes of this type have been probed mainly by infrared spectroscopy in solution[3] and in low temperature matrices.[4] The results of these experiments could, in principle, be modeled to provide information about the intermolecular potential of the complex, but it is often difficult to extract detailed information about the potential due to the complicated nature of the condensed phases. Hence it is desirable to obtain experimental information in the gas phase for an isolated complex.

In this paper, we present the results of molecular beam electric resonance spectroscopy on the species H_2CO–HF, which is the simplest example of a weakly bound complex formed between a carbonyl group and a strong protic acid. The main purpose of the experiment is to determine the structure of the complex at the minimum in the potential energy surface. The charge distribution of HF is relatively simple,[5] and it is roughly expected to behave as a dipolar probe of the charge distribution of formaldehyde, with the proton seeking out the electron-rich region of H_2CO. Based on simple molecular orbital pictures of formaldehyde,[6] two possible structural arrangements of H_2CO–HF are implied. If HF interacts with the highest π molecular orbital of H_2CO, the structure is expected to be t shaped with the HF axis perpendicular to the H_2CO plane and bisecting the CO axis, a structure analogous to that found for the π complexes C_2H_4–HF[7] and C_2H_4–HCl.[8] The other possiblity is an interaction with the n-type molecular orbitals associated mainly with the oxygen atom (the oxygen "lone pairs"), which would predict a bent, planar structure for the complex. If sp^2 hybridized orbitals exist, the $C = O \cdots H$ angle should be close to 120° for this second possibility.

Due to its relative simplicity, H_2CO–HF has also been the subject of a large number of theoretical investigations[9–16] dealing to various degrees with the question of the intermolecular potential surface of the complex. These studies all predict the planar structure to be more stable than the π-bonded structure, although the actual bond length and angle calculated for the planar structure varies considerably depending on the calculation.

EXPERIMENTAL

A molecular beam containing a specific complex can usually be formed by a supersonic nozzle expansion of the appropriate components seeded in Ar. However, even at low partial pressures, gaseous formaldehyde polymerizes in the presence of acid to form linear chains or polyoxymethylene $(CH_2O)_n$ as well as the cyclic species trioxane ($C_3H_6O_3$). Hence, a static gas mixture of HF, H_2CO, and Ar could not be used, and instead it was necessary to flow a mixture of 1% HF in Ar over

[a)]Supported by the National Science Foundation.

a heated sample of solid polyoxymethylene placed just before a stagnation chamber on which was mounted a 25 μm nozzle. The temperature of the nozzle and stagnation chamber was constantly maintained ~5 °C above the temperature of the sample container to prevent recondensation of formaldehyde polymers prior to the supersonic expansion. A sample temperature of ~55 °C and a stagnation pressure of 1.5–2.5 atm was used for all the experimental work. Under these conditions, the vapor pressure of H_2CO over the polymer sample[17] is ~0.035 atm. Hence the concentration of H_2CO present in the stagnation chamber was ~1.5%–2.5%. Maintaining the supersonic expansion at ~30 °C above ambient temperature did not seem to hinder complex formation nor did it measurably change the rotational temperature of the beam (assumed to be ~5–10 K when the expansion is run at 25 °C). This point will be discussed further below.

Although this source successfully produced enough of the desired complex for spectroscopic work, it did possess one minor drawback. Over several cycles of heating and cooling, the polymer sample would slowly deteriorate to give less gaseous formaldehyde at a given temperature. Possibly the surface area of the sample was decreasing over this period of time, causing the observed deterioration. In any case, it was necessary to replace the sample of polyoxymethylene approximately once a week to obtain enough formaldehyde in the gas phase to produce the complex.

TABLE I. Rotational transitions of H_2CO HF at zero electric field.

ν (MHz)[a]	$J'_{K_{-1}K_{+1}}-J_{K_{-1}K_{+1}}$	$F'-F$[b]
9 218.712(13)	$1_{01}-0_{00}$	2–1
9 218.793(18)		0–1
18 433.300(43)	$2_{02}-1_{01}$	
18 883.448(27)	$2_{11}-1_{10}$	2–1; 3–2; 2–2
18 883.527(24)		1–0
17 636.786(46)	$2_{12}-3_{03}$	
7 793.392(31)	$3_{13}-4_{04}$	
2 238.282(92)	$5_{05}-4_{14}$	
12 444.006(16)	$6_{06}-5_{15}$	
54 932.3(1)	$1_{11}-0_{00}$	
46 157.329(26)	$1_{10}-1_{01}$	
46 607.496(40)	$2_{11}-2_{02}$	
2 661.071(10)	$3_{12}-3_{13}$	
4 433.092(16)	$4_{13}-4_{14}$	
3.188(17)	$2_{20}-2_{21}$	
15.923(5)	$3_{21}-3_{22}$	
443.7531(8)	$1_{10}-1_{11}$	2–2; 1–1
443.7856(12)		1–2
443.8189(13)		1–0
443.754(2) (unsplit frequency)		
1 230.9285(14)	$2_{11}-2_{12}$	2–1
1 330.9483(14)		2–3
1 330.9725(27)		3–3; 2–2
1 330.9864(14)		2–2
1 331.0163(28)		1–2; 3–2
1 330.975(3) (unsplit frequency)		

[a]Uncertainties listed in parentheses are for the least significant digits and are obtained by dividing the linewidth at half-height by the siganl-to-noise ratio.
[b]The quantum number F is defined by $\vec{F}=\vec{J}+\vec{I}_H+\vec{I}_F$.

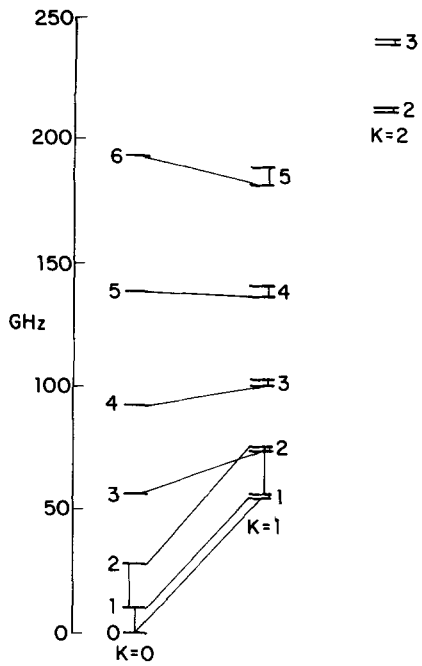

FIG. 1. Energy level diagram for H_2CO HF from 0 to 250 GHz. The transitions observed are shown by connections between energy levels. Not shown on the diagram are the levels 8_{18} and 8_{17} near 320 GHz which were observed under low resolution only.

A mass spectrometer, which is an integral part of the electric resonance detection scheme,[18] was used to monitor species present in the beam. A parent peak due to H_2CO–HF was present at m/e 50, but the complex was observed to crack predominantly to m/e 31 (H_2CO–H^+) and m/e 30 (H_2CO^+). Rotational resonances of H_2CO–HF were observed while monitoring either m/e 30 or m/e 31, and were not measurable with the mass spectrometer set to the parent peak. The best signal-to-noise ratio for H_2CO–HF resonances was obtained while monitoring m/e 30.

The rotational resonances measured for H_2CO–HF at zero electric field are collected and assigned in Table I. The standard rotational energy level labels for an asymmetric rotor are used,[19] where K_{-1} and K_{+1} correlate with the K quantum number of a limiting prolate and oblate symmetric top, respectively. The observed resonances imply that H_2CO–HF is a nearly prolate asymmetric rotor, so that K_{-1} is a reasonably good quantum number, giving the observed selection rules of $\Delta J = 0, \pm 1$ and $\Delta K_{-1} = 0, \pm 1$. Transitions following several different combinations of these selection rules were measured, providing enough information to determine all three rotational constants.

The rotational energy levels involved in the transitions listed in Table I cover a wide range (~0–250 GHz). An energy level diagram, with observed transitions shown is given in Fig. 1. This is the reason that a range in stagnation pressure (1.5–2.5 atm) is given above, rather than one value. For the transitions involving lower rotational energy levels, a higher stagnation pressure gave a better signal-to-noise ratio, while

TABLE II. Nonzero field measurements.[a,b]

Transition	V/cm	M_J	ν (MHz)
$1_{01}-0_{00}$	196.85	0–0	9226.755(9)
	246.06	0–0	9231.286(14)
	344.49	0–0	9243.344(12)
$1_{10}-1_{11}$	24.61	1–1	446.185(12)
	34.45	1–1	448.498(9)
	295.28	3	2675.787(17)
$3_{12}-3_{13}$	295.28	2	2667.240(11)
$\Delta M_J = 0$	393.70	3	2687.177(11)
	393.70	2	2672.040(15)
	393.70	4	4445.036(12)
	393.70	3	4441.324(25)
$4_{13}-4_{14}$	393.70	2	4438.660(13)
$\Delta M_J = 0$	393.70	1	4437.064(17)
	492.125	4	4451.748(19)
	492.125	3	4445.944(25)
	590.55	3	4451.596(25)
	319.88 (V/cm)		393.70 (V/cm)
	ν (MHz)	$M_F-M'_F$	ν (MHz)
	12.0276(32)	1–0	18.2497(32)
1_{01} Stark transition	12.0801(23)	1–2	18.3034(16)
$M_J-M'_J = 0-1$	12.1077(38)	0–1	18.3293(19)
	12.1389(21)	1–0	18.3615(17)
	12.1646(39)	0–1	18.3868(15)

[a]Uncertainties listed in parentheses are obtained as in Table I.
[b]M_F and M_J are the projections on the space-fixed axis of the angular momenta $\vec{F}$ and $\vec{J}$, respectively.

a lower stagnation pressure was optimal for transitions involving higher rotational energy levels. The signal-to-noise ratio for a rotational resonance depends on the populations in the two levels. Presumably, the rotational temperature, which determines the level populations, is inversely proportional to the stagnation pressure. This is in agreement with the experimental observation. The highest observable rotational energy level of the complex was determined to be ~320 GHz by measurement under low resolution of the $8_{18}-8_{17}$ asymmetry doublet at 15906 MHz (this frequency is not included in Table I). The next transition in the series, $9_{19}-9_{18}$, corresponding to an energy of 400 GHz could not be observed. This is roughly consistent with the presumed 10 K rotational temperature of the beam.

The dominant hyperfine splittings expected for this complex arise from interaction of the two spin 1/2 nuclei of HF with each other and with the magnetic field produced by the overall rotation. For most of the transitions observed in the microwave region (>3 GHz) the resolution (25 kHz) is not high enough to observe hyperfine splittings except in a few cases. Hence, the hyperfine interactions simply broaden the resonances and increase the measurement errors. For transitions observed in the radiofrequency region, where higher resolution is possible (1 kHz), resolved hyperfine spectra were obtained. The hyperfine transitions are assigned in Table I, where appropriate, with the quantum number F defined by $\vec{F} = \vec{J} + \vec{I}_H + \vec{I}_F$.

The measurements made in the presence of a static nonzero electric field are summarized in Table II. The Stark effect was measured for four of the rotational resonances, as well as the $J = 1$, $K_{-1} = 0$, $m_J = 0 \leftrightarrow 1$ Stark transition. The Stark effect measurements listed in Table II are sensitive to the two components (μ_a and μ_b) of the dipole moment of the complex resolved along the a and b inertial axes, despite the fact that they are all a-type transitions The $4_{13}-4_{14}$ resonance is particularly sensitive to μ_b because the 5_{05} rotational energy level is approximately halfway between the 4_{13} and 4_{14} levels, causing a strong b-type perturbation of the 4_{14} level and a strong c-type perturbation of the 4_{13} level. In fact, this three level system also provides a determination of μ_c. Two of the three possible transitions between the three levels are listed in Table I. It was a trivial matter to search for the third one, which is a c-type transition ($5_{05}-4_{13}$). The inability to see this transition (while the other two were quite strong) is firm experimental evidence that μ_c is zero.

As can be seen in Table II, hyperfine splittings due to HF were only resolved in the $J = 1$ Stark transition. This provides further information on the HF hyperfine interactions, which is complementary to the information provided by the zero-field measurements of the $1_{10}-1_{11}$ and $2_{11}-2_{12}$ asymmetry doublets.

Until now, the hyperfine interactions due to the formaldehyde protons have been ignored. This is because the direct nuclear spin–spin hyperfine interaction of H_2CO, which is expected to make the largest contribution to the rotational spectrum, is eight times smaller than the similar interaction in HF. Hence, splitting due to formaldehyde hyperfine interactions will not be resolvable in most of the rotational resonances. However, small hyperfine splittings due to formaldehyde were observed in measurement of the Stark transition of the $J = 1$, $K_{-1} = 0$ level. This is shown in Fig. 2. The quality of the spectrum shown in Fig. 2 is primarily due to lack of signal averaging. In particular to splitting of the line shown and the width of the lines is always observed in repeated spectra. Spectral enhancement by means of signal averaging was not used in this spectrum in order to avoid artificial broadening of the resonance due to long term drift of the electric field. The bottom portion shows the overall hyperfine pattern attributable to HF and documented in Table II. The linewidths observed in the spectrum (~10 kHz) are larger than usual for this frequency region. An attempt to measure the strongest component in the five line hyperfine pattern under higher resolution produced the spectrum shown in the upper portion of the figure, which clearly shows further splitting. This can only be attributed to the direct nuclear spin–spin interaction of formaldehyde. Actually, the linewidths observed in all of the high resolution measurements in the radiofrequency region were larger than expected, which can readily be explained by the presence of formaldehyde hyperfine splittings. The size of these splittings is close to the instrumental resolution, so that no quantitative measurements are recorded. However, the transition shown in Fig. 2 does prove that formaldehyde hyperfine structure is present in the rotational spectrum of the complex.

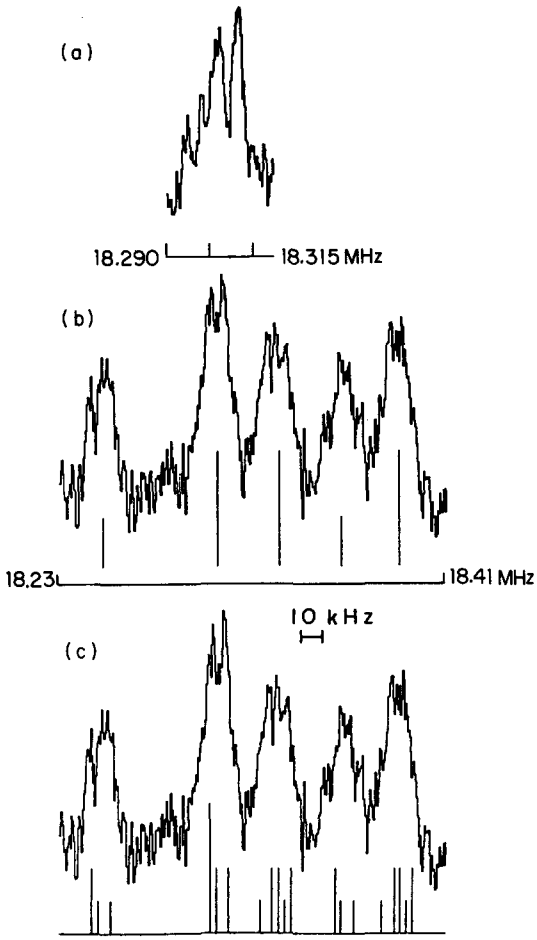

FIG. 2. $J=1$, $K_{-1}=0$. $M_J=0-1$ transition of H_2CO–HF at 393.7 V/cm. Single scan spectrum using 10 s time constant. (a) High resolution scan of the strongest component. The splitting observed is attributed to H_2CO hyperfine interactions. (b) and (c) Comparison of measured $J=1$, $K_{-1}=0$, $M_J=0-1$ transition at 393.7 V/cm with calculated spectrum. (b) Only HF hyperfine interactions included in the calculations. (c) H_2CO direct nuclear spin–spin coupling and HF hyperfine interactions included in calculation.

SPECTRAL ANALYSIS

In this section, the data presented in Tables I and II are used to obtain the rotational and distortion constants, the dipole moment, and the HF hyperfine constants of the H_2CO–HF complex. Since the hyperfine splittings are relatively insensitive to the rotational constants they can be analyzed separately. First we consider the rotational and distortion constant analysis.

The Hamiltonian describing the energy levels of a prolate asymmetric rotor, such as H_2CO–HF, is conveniently written for a symmetric rotor basis set as[20]

$$\mathcal{H} = \left(\frac{B+C}{2}\right)\bar{J}^2 + \left[A - \left(\frac{B+C}{2}\right)\right]K_{-1}^2 + \left(\frac{B-C}{2}\right)(\bar{J}_b^2 - \bar{J}_c^2) - \Delta_J(\bar{J})^2 - \Delta_{JK}\bar{J}^2K_{-1}^2 - \Delta_K K_{-1}^4 - 2\delta_J\bar{J}^2(\bar{J}_b^2 - \bar{J}_c^2) - 2\delta_K K_{-1}^2(\bar{J}_b^2 - \bar{J}_c^2) ,$$

where A, B, and C are the rotational constants, and Δ_J, Δ_{JK}, Δ_K, δ_J, and δ_K are the five centrifugal distortion constants defined by Watson.[21] Casting the Hamiltonian in this form provides guidance in the choice of parameters to be used in the least squares fitting procedure. This Hamiltonian also shows that since no $K_{-1}=1-2$ transitions were measured, the constants A and Δ_K cannot be determined separately. Hence, the data of Table I, after removal of the hyperfine splittings, is used to determine the constants $A-\Delta_K$, $B+C$, $B-C$, Δ_J, Δ_{JK}, δ_J, and δ_K, and these are collected in Table III.

The constants $B-C$ and δ_K are correlated (correlation matrix element >0.9), and this is reflected in their larger relative uncertainties compared to the other constants. All other constants are uncorrelated. Although the A rotational constant itself is not determined, Δ_K is not likely to be greater than 5 MHz. Hence the error in the A rotational constant is no larger than 0.01%, and this will have no discernable effect on the structure determination.

The usual perturbation treatment[20] of the Stark effect failed to account satisfactorily for the nonzero field measurements in Table II. Hence, the Stark shifts were calculated by adding to the rotational Hamiltonian given above the following Stark Hamiltonian[18]:

$$\mathcal{H}_S = -E_a\mu_a S_{aa} - E_b\mu_b S_{ba} .$$

Here E_a is the space fixed electric field, and the S_{ia} are elements of the direction cosine matrix used to transform from space-fixed to molecule-fixed axes. The matrix of the total Hamiltonian $\mathcal{H}+\mathcal{H}_S$ was set up in a symmetric rotor basis set, truncated for J values exceeding the J of interest by two, and diagonalized to obtain the energy levels of the complex in the presence of an electric field. Least squares fitting procedures were then used to determine μ_a and μ_b.

Table IV summarizes the results of the Stark effect analysis. The dipole moment components of the complex, the resultant total dipole moment, and for comparison, the dipole moments of the individual submolecules are listed in the table. μ_a and μ_b were determined from the data in Table II, and μ_c was experimentally shown to be zero as discussed in the previous section.

The hyperfine splittings present in the rotational spectrum of the complex are now considered. The hyper-

TABLE III. Rotational and distortion constants of H_2CO–HF.[a]

MHz	
$A-\Delta_K=50\,543.205(23)$	$\Delta_J=0.0380(2)$
$B+C=9218.853(8)$	$\Delta_{JK}=-0.838(5)$
$B-C=445.611(65)$	$\delta_J=0.006\,03(3)$
$B=4832.232$	$\delta_K=0.452(16)$
$C=4386.621$	
$\kappa=-0.98$	$\Delta=0.62$ amu Å^2

[a]Uncertainties in parentheses are obtained from statistical analysis and are adjusted to give 95% confidence levels.

TABLE IV. Dipole moment of H_2CO–HF (D).[a]

$\mu_a = 3.7535(2)$	$\mu^{H_2CO} = 2.332$[b]
$\mu_b = 1.399(1)$	$\mu^{HF} = 1.8265$[c]
$\mu_c = 0$	
$\mu = 4.006$	

[a]Uncertainties in parentheses are obtained from statistical analysis and are adjusted for 95% confidence levels.
[b]B. Fabricant, D. Krieger, and J. S. Muenter, J. Chem. Phys. **67**, 1576 (1977).
[c]J. S. Muenter and W. Klemperer, J. Chem. Phys. **52**, 6033 (1970).

fine interactions most likely to produce observable splittings in the spectra are the direct nuclear spin–spin coupling in HF and in H_2CO, and the spin rotation coupling of the hydrogen and fluorine nuclei of HF. The other possible hyperfine interactions, such as the hydrogen spin-rotation coupling of H_2CO and the electron coupled nuclear spin–spin interaction in HF, are too small (< 0.5 kHz) to be detected in our experiment.

The hyperfine Hamiltonian needed to calculate the spectra is[20]

$$\mathcal{H}_{hfs} = C_H \bar{I}_H \cdot \bar{J} + C_F \bar{I}_F \cdot \bar{J} + \mathcal{H}^{HF}_{sp-sp} + \mathcal{H}^{H_2CO}_{sp-sp} ,$$

where the form of the spin–spin Hamiltonian for either HF of H_2CO is

$$\mathcal{H}_{sp-sp} = \frac{2[S_a(\langle J_c^2\rangle - \langle J_a^2\rangle) + S_b(\langle J_c^2\rangle - \langle J_c^2\rangle)]}{J(J+1)(2J-1)(2J+3)} \times [3(\bar{I}_1 \cdot \bar{J})(\bar{I}_2 \cdot \bar{J}) + 3(\bar{I}_2 \cdot \bar{J})(\bar{I}_1 \cdot \bar{J}) - 2(\bar{I}_1 \cdot \bar{I}_2)\bar{J}^2] .$$

C_H and C_F are the spin-rotation constants for HF in the complex, and S_a and S_b are diagonal elements of the direct nuclear spin–spin coupling tensor.

The transitions to be analyzed are the 1_{10}–1_{11} and 2_{11}–2_{12} asymmetry doublets and the $m_J = 0 - 1$ Stark transition in the 1_{01} level. Since the hyperfine energies are much smaller than the rotational energies, the hyperfine splittings for the four $K_{-1} = 1$ energy levels were calculated using $\mathcal{H}_{hfs}$ and simply added to the rotational energy of each level. Similarly, since the Stark transition is in the strong field limit, hyperfine splittings for it were calculated using a Hamiltonian consisting of $\mathcal{H}_{hfs}$ plus a simple Stark energy term appropriate for the $K = 0$ level of a prolate symmetric top with one dipole moment component. The dipole moment fitting parameter was adjusted to give the correct frequency shift.

We consider first the Stark transition. The hyperfine splittings here are sensitive mainly to the value of S_a^{HF} and are affected slightly by the value of $S_a^{H_2CO}$. The splittings are insensitive to the values of the spin-rotation constants. Hence the hyperfine calculations are performed by fixing C_H, C_F, and $S_a^{H_2CO}$ at appropriate values. S_a^{HF} is then adjusted to reproduce the observed hyperfine splittings.

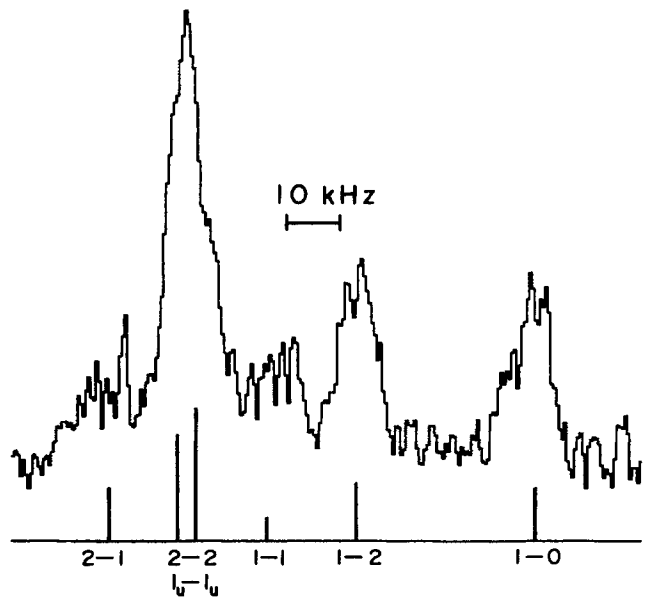

FIG. 3. Measured 1_{10}–1_{11} transition at zero field showing HF hyperfine splittings. This represents a scan of the region 443.72–443.85 MHz. The numbers underneath the calculated spectrum indicate the F quantum number changes involved with $\bar{F} = \bar{J} + \bar{I}_H + \bar{I}_F$. The designation 1_u simply serves to distinguish the two $F = 1$ hyperfine components of each rotational level.

In Fig. 2, the Stark transition is compared with two different calculations of the hyperfine spectrum. The top part of the figure shows the result when only HF hyperfine effects are considered, while the bottom part shows the result when the formaldehyde direct nuclear spin–spin coupling is included. Clearly, the inclusion of H_2CO hyperfine accounts for the broad linewidths observed in the spectrum and for the small splitting which was partially resolved in the largest component. Furthermore, a careful examination of either the observed spectrum or the line centers recorded in Table II shows that the spacings between the four high frequency components are better accounted for when H_2CO hyperfine is included in the analysis. These spacings are equal when only HF hyperfine effects are present. Hence, even though the formaldehyde hyperfine interaction is small and nearly unresolvable, its effect on the Stark transition is noticeable and produces slight shifts (~1 – 2 kHz) in the line positions.

The hyperfine splittings in the asymmetry doublets are sensitive to both S_a^{HF} and S_b^{HF} and slightly sensitive to C_H and C_F. The formaldehyde hyperfine can be neglected in this case, because its inclusion in the calculation does not measurably alter the line positions. Figure 3 shows the measured 1_{10}–1_{11} asymmetry doublet spectrum, along with the calculated spectrum. C_H and C_F are fixed in the calculation, as before, and S_a^{HF} and S_b^{HF} are adjusted to reproduce the observed splittings. Since S_a^{HF} is well determined from the Stark transition, the zero field hyperfine spectra basically determine the value of S_b^{HF}.

Table V summarizes the hyperfine constants of

TABLE V. Hyperfine constants of H_2CO–HF.[a,b]

$S_a = 93.60(84)$	$\langle\cos^2\theta_a\rangle = 0.7686(39)$	
$S_b = -31.7(11)$	$\langle\cos^2\theta_b\rangle = 0.1861(52)$	
	$\langle\cos^2\theta_c\rangle = 0.0453(65)$	
Fixed in least-squares fitting procedure[c]		
	$M_a^F = -1.34$	$M_a^H = 5.81$
$S_a^{H_2CO} = 9.39$	$M_b^H = -0.45$	$M_b^F = 1.96$
$S_b^{H_2CO} = -0.547$	$M_c^H = -0.48$	$M_c^F = 2.09$

[a]Uncertainties obtained for S_a and S_b are derived from least-squares fitting procedure and adjusted for 95% confidence levels. The angular expectation values are derived using formulas given in the Appendix.
[b]All hyperfine constants are given in kHz.
[c]M_g^I is the spin rotational constant for the I nucleus along the g inertial axis.

H_2CO–HF. S_a^{HF} and S_b^{HF} were determined by a weighted nonlinear least squares analysis of the combined zero and nonzero field data. None of the residuals obtained in this fit were larger than the measurement errors, and the fitting parameters were uncorrelated. Also included in Table V are average values for the squares of the direction cosines of the HF axis with respect to the a and b inertial axes. Finally, the parameters used to fix the spin-rotation constants and the H_2CO spin–spin coupling constant in the least squares fit are listed in the table.

Before leaving the analysis of the hyperfine spectra, we wish to indicate more quantitatively the sensitivity of the spectra to the fixed parameters C_H, C_F, and S_a^{H2CO} In the case of the Stark transition, neglect of all hyperfine interactions except the HF nuclear spin–spin coupling changes the determined value of S_a^{HF} in Table V by 1%. In the case of the zero field spectra, a change of 50% in C_H and C_F would change the value of S_b^{HF} obtained by 7%. The corresponding change in the angle θ_b derived from S_b^{HF} would be 7°. On the other hand, a 50% change in the values of C_H and C_F would not reproduce the observed spectra to within the measurement errors, lending confidence to the values of C_H and C_F derived from the scaling relations.[22,23]

AVERAGE STRUCTURE

A structural model for the H_2CO–HF complex which is consistent with the spectroscopic constants obtained in the previous section is now derived. As usual, the description of a molecular system in terms of a rigid structure must be properly defined, due to the ever present zero point oscillations of the individual atoms, which become even larger in a weakly bound complex. The structural parameters derived below are obtained from state vibrational modes of the complex. As such they complex in the ground state.

The five structural parameters required to model the average geometry of the complex are defined in Fig. 4. $r_{c.m.}$ is the distance between the centers of mass of the submolecules, χ is the angle made by the C_2 symmetry axis of formaldehyde with the center of mass line, γ is the analogous angle made by HF, ϕ_1 is the angle defining rotation about the C_2 axis in formaldehyde ($\phi_1 = 0°$ gives a planar arrangement), and ϕ_2 is the dihedral angle of the HF axis with respect to the C–O axis ($\phi_2 = 0°$ is defined to place the CO and HF axes in the same plane with the oxygen and hydrogen atoms on the same side of the center of mass line). In this model, we assume that the bond lengths and bond angles of the isolated submolecules are unchanged on complex formation.

The rotational constants give the average moments of inertia of the molecule, which are mainly determined by the heavy atom positions. The parameters $r_{c.m.}$ and χ are found to be most sensitive to the constants $B + C$ and A, respectively. These constants alone establish two possible heavy atom orientations, corresponding to structures with an angle of χ (oxygen closer to fluorine) and $180° - \chi$ (carbon closer to fluorine). The latter structure can be ruled out immediately. For a planar arrangement of formaldehyde ($\phi_1 = 0°$), one of the H_2CO protons would be situated unreasonably near the HF molecule for this structural possibility, while a nonplanar arrangement ($\phi_1 = 90°$) is ruled out by the inertial defect, as discussed below. Thus, the heavy atom orientation shown in Fig. 4 is the correct one. The inertial coordinate system depicted in the figure is basically established by the heavy atom locations.

Since the protons are light, their average positions are harder to establish from the measured rotational constants alone. Fortunately, other spectroscopic constants, provide detailed information about the average orientation of the HF axis in the complex with respect to the inertial axes. Because both submolecule dipole moments are large in this case, the usual ambiguities arising from dipole induction effects are not important, and the magnitude of the dipole moment components roughly establishes the orientation of the HF axis. Hence, the large value of μ_a shows that the projections of the submolecule dipole moments onto the a axis must be additive. This requires the HF hydrogen to point towards the formaldehyde submolecule.[24] The relatively small value of μ_b indicates that the b-axis projections of the submolecule dipole moments must subtract.[25] This requirement further restricts the HF hydrogen to be on the same side of the a axis as the oxygen atom, giving the orientation depicted in Fig. 4.

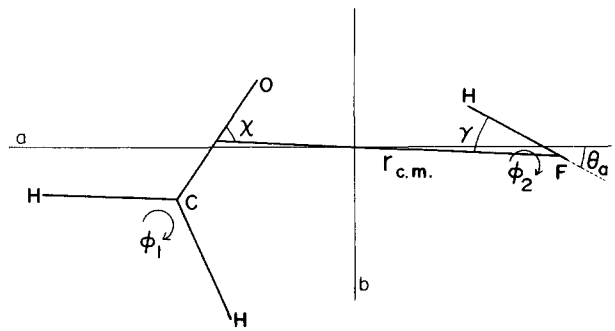

FIG. 4. Definition of coordinates required to describe H_2CO–HF structure.

TABLE VI. Effect of variation of ϕ_1 on structure determination.[a]

ϕ_1	$r_{c.m.}$ (Å)	χ	γ	$\pm\phi_2$	Δ (amu Å^2)	$B-C$ (MHz)
0	2.8741	58.92	26.3	29.4	−0.08	416
15	2.8740	58.48	26.4	31.5	−0.30	407
30	2.8736	57.33	26.4	33.5	−0.93	381
45	2.8731	55.87	26.3	34.9	−1.80	344
90	2.8722	53.31	25.7	30.5	−3.70	264

[a]All angles are given in degrees.

The angular expectation values derived from the HF hyperfine constants and listed in Table V now provide a quantitative measure of the average HF orientation. The angle θ_a defines a cone of possible HF orientations about the a axis, while the angle θ_b defines a similar cone about the b axis. Clearly, the intersection of these cones gives the average position of HF in the complex. Note that the cones intersect for two equivalent positions above and below the $a-b$ plane. This is to be expected since both in-plane and out-of-plane oscillations of HF about its center of mass occur, giving an average nonplanar HF orientation. The magnitude of the average out-of-plane angle obtained from θ_a and θ_b is equivalent to the angle obtained from $\langle\cos^2\theta_c\rangle$, since $\langle\cos^2\theta_a\rangle + \langle\cos^2\theta_b\rangle + \langle\cos^2\theta_c\rangle = 1$. [$\theta_c$ is found to be 77.7(9)° and the angle HF makes with the $a-b$ plane is 12.3(9)°.]

All the structural parameters have now been discussed except ϕ_1, which is related to the H_2CO hydrogen positions. The other spectroscopic constant, $B-C$, can be used to determine a likely value of ϕ_1. We consider the effect of varying the angle ϕ_1 on the structure and inertial constant determination in Table VI. Here, for a given value of ϕ_1, the structural parameters $r_{c.m.}$, χ, γ, and ϕ_2 are adjusted to reproduce the spectroscopic constants $B+C$ and A, and the average angles θ_a and θ_b. The structural parameters thus obtained, as well as the inertial defect Δ and spectroscopic constant $B-C$ appropriate for the given structure, are listed for values of ϕ_1 in the range 0°–90°. Plus and minus values of ϕ_2 are indicated in the table to emphasize that out-of-plane oscillations of the HF axis give equal probability of finding the hydrogen atom above and below the $a-b$ plane on average. As can be seen in the table, variation of the angle ϕ_1 only affects the determination of χ to a noticeable extent. The other structural parameters are relatively insensitive to it. Both the inertial defect and $B-C$, which are really just alternate measures of the same thing, are quite sensitive to ϕ_1. Hence, the best agreement with experimental observables occurs when $\phi_1 = 0°$, i.e., the planar structure. Of course, zero point oscillations of the formaldehyde submolecule are expected, and, on average, ϕ_1 is likely to be different from 0°. There is unfortunately no experimental probe of the oscillation amplitude, but we expect it to be in the range 15°–25°.

In Table VII we collect the average structural parameters of H_2CO–HF calculated with ϕ_1 fixed at 0°. The uncertainties listed for the parameters are derived from uncertainties in the measured spectroscopic constants. The model error due to keeping ϕ_1 fixed at 0° is larger than these uncertainties and can be gleaned from Table VI. Note that θ_a and θ_b for HF are obtained from HF hyperfine measurements, while θ_a and θ_b for H_2CO are obtained from the fit to A and $B+C$. The O–H weak bond length, the C=O···H angle, and the C=O···F angles are also included in the table. The projection onto the $a-b$ plane of the average structure defined by these parameters is drawn to scale in Fig. 4.

Finally, one other experimental observation provides information relevant to the structural model of H_2CO–HF. The observation that formaldehyde hyperfine structure is present in the rotational spectrum of the complex is of importance in establishing the degree of nonrigidity of the molecule. The interchange of the two formaldehyde protons produces two equivalent structures. Hence, besides the usual large amplitude motions expected in a weakly bound system, it is also possible that tunneling occurs in this complex. Presumably, there is a barrier to the rotation of the formaldehyde submolecule about its C_2 axis (since the nature of the weak bond is altered). Hence the potential energy for such motion is conveniently written as a function of ϕ_1, and will qualitatively resemble a symmetric double well potential with minima occurring at $\phi_1 = 0°$ and 180° and a maximum at $\phi_1 = 90°$.

The characteristic energy levels and wave functions of systems described by such potentials have been discussed.[26] Basically, the energy levels occur in closely spaced pairs, with the lowest energy pair separated by the least amount. As the barrier height increases, the separation between the pairs decreases (i.e., the energy levels occur in degenerate pairs for an infinite barrier) and the tunneling rate also decreases. The ground state wave function ψ_0 is symmetric, with two maxima occurring at $\phi_1 = 0°$ and 180°. Because of tunneling, ψ_0 gives a nonzero probability of finding the system with $\phi_1 = 90°$. As the barrier height increases, this probability decreases. The wave function ψ_1 corresponding to the higher energy level in the lowest energy pair, is antisymmetric, with a node at 90°. Because of the different behavior of ψ_0 and ψ_1 at $\phi_1 = 90°$, the average

TABLE VII. Average structural parameters of H_2CO–HF.[a]

$r_{c.m.}$ (Å)	2.87413(1)	r_{O-H} (Å)	1.7935
χ	58.92(3)	r_{O-F} (Å)	2.6588
γ	26(1)	∠C=O···H	115
ϕ_2	±29(3)	∠C=O···F	109.5
ϕ_1	0 (fixed)	θ_a (HF)	28.75
		θ_b (HF)	64.4
		θ_c (HF)	77.7
		θ_a (H_2CO)[b]	56.1
		θ_b (H_2CO)[b]	33.9

[a]All angles are given in degrees.
[b]θ_a (H_2CO) and θ_b (H_2CO) are angles made by the C_2 axis.

rotational constants of the complex associated with the two states will be different (the difference in rotational constants for the two structures with $\phi_1 = 0°$ and $\phi_1 = 90°$ is $\Delta A = 5795$ MHz, $\Delta B = 25.9$ MHz, and $\Delta C = -72$ MHz). As the barrier height increases, the difference between the two sets of rotational constants decreases.

The rotation described by ϕ_1 in the complex correlates with rotation about the C_2 axis in free formaldehyde (which corresponds to K_{-1} excitation). Hence, ψ_0 correlates with the even K_{-1} rotational wave functions of H_2CO, while ψ_1 correlates with the odd K_{-1} rotational wave functions of H_2CO. We can now use the known spin states corresponding to the odd and even K_{-1} levels in H_2CO, to establish that ψ_0 goes with the singlet formaldehyde spin state while ψ_1 goes with the triplet formaldehyde spin state.

The observation of splittings in the rotational spectrum of the complex attributable to formaldehyde hyperfine interactions thus shows that the upper tunneling state ψ_1 is populated in the beam. Clearly, the lower tunneling state must also be present. However, the microwave spectrum shows no evidence, to the level of resolution available, of splitting due to the presence of two tunneling states with slightly different rotational constants. It must hence be assumed that the barrier to tunneling in the complex is relatively high, and that therefore the two sets of rotational constants for the tunneling states do not differ by more than a few kHz.

We estimate a lower limit for the barrier hindering simple rotation of the formaldehyde submolecule about its C_2 symmetry axis with moment of inertia I^0, (I^0 is I^a of H_2CO). For the potential we use the simple symmetric splicing of two harmonic forms about the equivalent planar equilibrium configurations.[26] For this model the force constant (energy rad^{-2}) is $k = 8V_0/\pi^2$, with V_0 the barrier height.

The difference in expectation value of a positional operator $O(\Theta)$ between lowest symmetric and antisymmetric starts in this model is

$$O_+ - O_- = \exp\left\{\frac{-\pi^2 V_0 I^0}{h^2}\right\}[O(\pi/2) - O(0)] .$$

The rotational constant showing the greatest difference between planar and perpendicular orientation of H_2CO in the complex is A. From Fig. 1 and Table I it is seen that a number of transitions observed involve A. Clearly we may state experimentally that $|A_+ - A_-| < 100$ kHz. This gives a limit $V_0 > 500$ cm^{-1}.

In recent work on H_2S–HF,[26] hyperfine splittings in the $J = 1$, $K_{-1} = 0$ Stark transition due to the presence of the triplet spin state of H_2S were observed, similar to the observations in the present work. However, in the H_2S–HF study, the authors come to a different conclusion regarding the tunneling problem. The interpretation given assumes that the barrier to tunneling is low, and that splittings due to the presence of the two tunneling states should be observed in the microwave spectrum. Since no splittings were observed, however, the authors assume that the lower energy tunneling level corresponding to the singlet spin state of H_2S is not present in the beam. This result is puzzling to us since the rotational constants and dipole moment of the singlet spin system should be similar to the triplet spin system.

INTERNAL DYNAMICS

The distortion constants determined for H_2CO–HF contain information about its internal force field. Unfortunately, there are 12 vibrational degrees of freedom in H_2CO–HF, and the number of force constants associated with these exceeds the available information content of the measured distortion parameters. However, since some distortion constants depend mainly on one force constant, a limited amount of information can be obtained. In particular, if the internal vibrations of the submolecules are neglected, then the force constant f_s associated with stretching the molecular along the center of mass line is determined from the distortion constant τ_{cccc}.

Both distortion constants τ_{bbbb} and τ_{cccc} are related to the measured constants Δ_J and δ_J by[20]

$$\hbar^4 \tau_{bbbb} = -4h(\Delta_J + 2\delta_J) ,$$

$$\hbar^4 \tau_{cccc} = -4h(\Delta_J - 2\delta_J) .$$

The τ's are related to the force constants and inertial derivatives of the complex in the following way:

$$\tau_{\alpha\alpha\alpha\alpha} = -\frac{1}{2}\frac{1}{I_\alpha^4}\sum_{i,j}\left(\frac{\partial I_\alpha}{\partial R_i}\right)\left(\frac{\partial I_\alpha}{\partial R_j}\right)(f^{-1})_{ij} ,$$

where R_i are the internal coordinates and f^{-1} is the inverse of the force constant matrix. For the nearly planar arrangement of H_2CO–HF, I_c is given to a good approximation by $I_c = I^{HF} + I_3^{H_2CO} + M_s r_{c.m.}^2$, where I^{HF} is the moment of inertial of HF, $I_3^{H_2CO}$ is the moment of inertial about the c axis of H_2CO, and M_s is the reduced mass given by $M_s = (M_{HF})(M_{H_2CO})/(M_{HF} + M_{H_2CO})$. I_b turns out to be a more complicated function of $r_{c.m.}$, χ, and γ. Hence, in the expression relating τ_{cccc} to the force constants, all terms except the one involving f_s are approximately zero, whereas terms involving the other internal coordinates contribute to τ_{bbbb}. Using $\partial I_c/\partial r_{c.m.} = 2M_s r_{c.m.}$, the expressions given above readily provide a value for $(f^{-1})_{r_{c.m.}}$. If the interaction force constants can be neglected, the reciprocal of this gives a value of f_s. We obtain $f_s = 0.088$ mdyn/Å. The associated vibrational frequency is $\nu_s = (1/2\pi)\sqrt{f_s/M_s} = 110$ cm^{-1}.

The average out-of-plane orientation of the HF axis determined above provides a measure of the vibrational amplitude for the out-of-plane motion. Assuming that the motion can be described by simple harmonic oscillation, the vibrational frequency can be approximated from the amplitude.[29] Hence,

$$\langle\theta^2\rangle = \frac{h}{8\pi^2 M_b \nu_b} ,$$

where M_b, the reduced mass for the bend, is approximated by the moment of inertia of HF, and $\langle\theta^2\rangle$ is the expectation value for the square of the amplitude. Use of the measured out-of-plane orientation provides the estimate $\theta = 12.3°$. Hence the vibrational frequency

associated with the out-of-plane bending of the HF molecule against the H_2CO submolecule is $\nu_b = 420$ cm^{-1}. The force constant for this vibration is $k_b = 0.09$ mdyn Å. We must insert the caution that these vibration frequencies are dependent upon our model for the force field and can contain errors greater than those present in the centrifugal distortion coefficients.

DISCUSSION

The structural results obtained for the gas-phase complex H_2CO–HF can be put in perspective by comparison with some other weakly bound HF complexes. Table VIII compares structures, force constants, and dipole moment enhancements of four such complexes studied by molecular beam electric resonance techniques (the dipole moment enhancement of H_2CO–HF is derived below). Note that all four complexes involve a hydrogen bond to unsaturated oxygen. The most puzzling feature of the comparison concerns the varied weak bond angles found for the four species. Simple models of the interaction do not account for the differences in the observed stereochemistry. For example, a simple electrostatic model would predict an angle of 180° in all four cases, since dipole–dipole and dipole–quadrupole interactions favor a linear arrangement in these examples. In fact the strongest possible dipole–dipole interaction occurs in the case of H_2CO–HF, where both submolecules possess very large dipole moments. Yet, of the four complexes, the weak bond angle in H_2CO–HF deviates the most from the 180° angle expected from electrostatic considerations. On the other hand, the strength of the interaction, as probed by the weak bond lengths and the force constants, is in rough agreement with the prediction of the electrostatic model; i.e., the strongest interaction does seem to occur in H_2CO–HF. Simple molecular orbital pictures also fail to account for the angular variation. Most models for the orbitals associated with an unsaturated carbon–oxygen bond place the π-electron density perpendicular to the bond and the nonbonding electron density in lone-pair orbitals pointing ~120° away from the C–O bond. (N_2O is isoelectronic to CO_2 and its calculated MO's are very similar to those for CO_2.) If HOMO-LUMO interactions are invoked, all four species in Table VIII should have bent structures, and the X=O···F angles should be close to 120°. Clearly, this is not observed to be the case, although it is interesting that the angles appear reasonably close to the expected value of 120° for the two bent species. If the HF molecule can be thought of as a probe of the electron-rich region in the four submolecules, the results of Table VIII indicate that the charge distribution around the unsaturated oxygen in the four cases does not in general follow the simple molecular orbital pictures outlined above.

Kollman[30] has considered a theory of hydrogen bond directionality in which electrostatic and charge transfer considerations are used together as a guide in establishing stereochemistry. Since charge transfer is optimal in the geometry which favors maximum overlap of the interacting molecular orbitals, Kollman's model is basically a combination of the two models described above. Hence, the minimum energy geometry in hydrogen bonded complexes represents a balance between electrostatic and charge transfer effects. In general, as the hydrogen bond length decreases, the charge transfer contribution should become more important. Since the bond length is much shorter in H_2CO–HF than in CO_2–HF, the charge transfer contribution is thought to be more important in the former, and a bent structure is favored for it. This rationalization appears consistent with the results for the three C=O···H bonds, but does not account for the N_2O–HF result. Basically, the observed stereochemistry of the four complexes remains unaccounted for on the basis of the simple models for the interaction discussed here.

TABLE VIII. Comparison of weakly bound complexes containing HF bound to unsaturated oxygen.

Parameter	H_2CO–HF	CO_2–HF[a]	SCO–HF[a]	NNO–HF[b]
r_{O-H} (Å)	1.79	1.91	1.94	1.94
∠X=O···F (deg)	110	~180	~180	116
k_s (mdyn/Å)	0.088	0.021	0.028	···
k_b (mdyn/Å)	0.09	0.022	0.02	···
$\Delta\mu_a$ (D)[c]	0.86	0.60	0.84	0.50

[a]F. A. Baiocchi, T. A. Dixon, C. H. Joyner, and W. H. Klemperer, J. Chem. Phys. **74**, 6544 (1981).
[b]C. H. Joyner, T. A. Dixon, F. A. Baiocchi, and W. Klemperer, J. Chem. Phys. **74**, 6550 (1981).
[c]The dipole moment enhancement is defined in the text.

One other puzzling feature in the comparisons of Table VIII concerns the dipole moment enhancement. A large value for this quantity is found in all four species, despite the fact that a fairly large difference in interaction strengths (as measured by the bond lengths and force constants) is observed between H_2CO–HF and the other three complexes. Clearly, there seems to be no correlation between the strength of the interaction and the charge distortions that occur. The dipole moment enhancements cannot be accounted for in any of the four species by consideration of an electrostatic model alone. The effect of charge transfer on the dipole moments is also difficult to model reliably.

The theoretical studies of H_2CO–HF given in Refs. 9–16 agree roughly with the observed structure, in that all the studies predict the bent, planar structure to be the lowest energy form of the complex. Actual bond lengths and angles are in poor agreement with the structure observed here. The range in calculated O–H bond lengths is 1.80–1.34 Å (1.79 Å observed), while the range in C=O···F angles calculated is 120°–140° (110° observed). None of the calculations were apparently able to predict the unexpectedly small C=O···F angle observed. Finally, the theoretical studies all predict (or assume) that the hydrogen bond is linear. The present experiment indicates that, at least in the average structure, the hydrogen bond deviates from linearity by ~10°. This point is of some significance and will be discussed in more detail later.

Comparison of the structures of isolated complexes

with the structures of corresponding crystals is of interest in elucidating the difference in the intermolecular forces present in the two phases. Unfortunately, direct comparison of our result with crystals containing hydrogen bonds of the form C=O···HF is not possible. However, a large amount of x-ray and neutron diffraction work has been carried out on crystals containing hydrogen bonds of the form C=O···H–O. This work has been reviewed by Olovsson and Jönsson.[2]

The values found for the C=O···H angles scatter widely about an average value of ~120°. The O···H–O angles are usually close to 180°, but small deviations (~10°) from this value are common. The result for acetic acid[31] provides a typical example of the structural parameters found for a hydrogen bond to a carbonyl group in the solid phase. The hydrogen bond length in acetic acid is found to be 1.64 Å, a value 0.15 Å shorter than the hydrogen bond length of H_2CO–HF. This difference is most likely attributed to close packing in the crystal, rather than to a stronger hydrogen bond in acetic acid. The hydrogen bond angles obtained in acetic acid show a deviation of 9° from the linear hydrogen bond arrangement. Specifically, for the C=O···H–O linkage in solid acetic acid, the C=O···O angle is found to be 123°, while the C=O···H angle is found to be 129°. This can be compared with the average structure of H_2CO–HF, for which the C=O···F angle is 109.5° and the C=O···H angle is 115.2°. Apparently, the unexpectedly small hydrogen bond angle found for the isolated species H_2CO–HF is not found in hydrogen bonded crystals of acetic acid. Again, this difference most likely reflects the restrictions imposed on the hydrogen bond angles by the requirements of close packing in the crystal. In the isolated complex, the submolecules can orient themselves to maximize the attractive interactions.

There is ample evidence of nonlinear hydrogen bonds in structural studies on crystals. Whether or not this is favored by the hydrogen bond interaction itself or by the requirements of the crystal lattice is unclear. The average structure of H_2CO–HF determined from its microwave spectrum also implies a nonlinear hydrogen bond. In this case, however, the uncertainties present in the results for the condensed phase do not affect our conclusion. The only ambiguity present in the gas phase result concerns the effect of the vibrational motions on the structure determination. In other words, a nonlinear hydrogen bond in the average structure does not necessarily rule out a linear hydrogen bond in the equilibrium structure. To determine the equilibrium orientation of the HF axis, we must model the vibrational motions in the molecule. The vibrational amplitudes of the heavy atoms are smaller than those of the hydrogen atoms, hence the equilibrium heavy atom orientation is probably not too far from the average orientation determined above. To model the HF oscillation, we assume that the amplitudes for the in-plane and out-of-plane motions are the same. This assumption is supported by the far infrared spectrum of H_2CO–HF obtained in a low temperature argon matrix,[33] which shows that the vibrational frequencies associated with the HF librations are nearly degenerate. The frequencies are 602 and 612 cm^{-1}, giving a ratio of $\sqrt{612/602} = 1.01$ for the amplitudes of the two motions. The agreement between the frequencies measured in the Ar matrix and the frequency estimated above from the average out-of-plane orientation (420 cm^{-1}) is not good, but this may not be a fair comparison since the methods used to obtain the frequencies are so different.

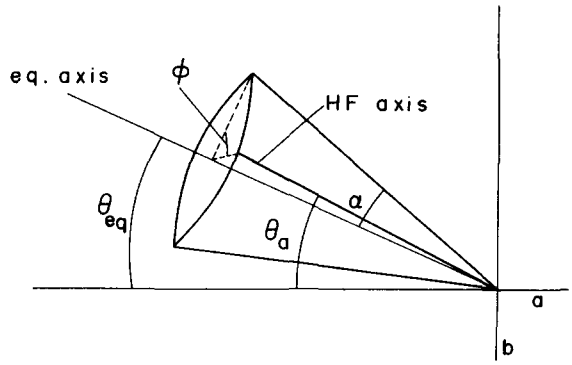

FIG. 5. Definition of angles required to model isotropic oscillation of the HF axis about an HF equilibrium orientation.

The model used to describe the HF vibration is shown in Fig. 5. The HF molecule is assumed to oscillate isotropically about its center of mass to produce a cone of possible HF orientations about the equilibrium axis, where the cone angle α represents the vibrational amplitude of the degenerate oscillation. An instantaneous HF axis orientation on this cone is given by specifying the angle ϕ. The direction cosines defining the HF axis orientation with respect to the a, b, and c inertial axes may be written for an instantaneous orientation using trigonometric identities. The following relations are obtained:

$$\cos\theta_a = \cos\alpha\cos\theta_{eq} - \sin\alpha\sin\theta_{eq}\cos\phi ,$$

$$\cos\theta_b = \cos\alpha\sin\theta_{eq} + \sin\alpha\cos\theta_{eq}\cos\phi ,$$

$$\cos\theta_c = \sin\alpha\sin\phi .$$

When ϕ is averaged out of these expressions, we obtain the dependence of the average direction cosines on the amplitude and equilibrium orientation:

$$\langle\cos\theta_a\rangle = \cos\alpha\cos\theta_{eq} ,$$

$$\langle\cos\theta_b\rangle = \cos\alpha\sin\theta_{eq} ,$$

$$\langle\cos\theta_c\rangle = 0 .$$

Similar averages are easily obtained for the squares of the direction cosines:

$$\langle\cos^2\theta_a\rangle = c\cos^2\alpha\cos^2\theta_{eq} + \tfrac{1}{2}(\sin^2\alpha\sin^2\theta_{eq}) ,$$

$$\langle\cos^2\theta_b\rangle = \cos^2\alpha\sin^2\theta_{eq} + \tfrac{1}{2}(\sin^2\alpha\cos^2\theta_{eq}) ,$$

$$\langle\cos^2\theta_c\rangle = \tfrac{1}{2}(\sin^2\alpha) .$$

The angular expectation values obtained from the HF hyperfine constants can be used immediately to solve for α and θ_{eq}. We obtain an amplitude of $\alpha = 17.5(1.3)°$ and an equilibrium orientation of the HF axis with respect to the a axis of $\theta_{eq} = 23.8(7)°$, where the uncertainties are derived from uncertainties in the hyperfine constants. The corresponding equilibrium angle ob-

tained when the HF axis is required to point at the oxygen atom is $\theta_{eq} = 14°$. Hence, this model predicts that the hydrogen bond in the equilibrium structure of H_2CO–HF deviates by 10° from linearity.

In using this model, the CO and HF axes have been assumed coplanar in the equilibrium structure. This is a reasonable assumption since the c-axis component of the dipole moment is found to be zero. The effect of H_2CO oscillation was also neglected in this model. Motion of the H_2CO submolecule would affect the HF orientation with respect to the a axis, thus making θ_{eq} a function of H_2CO vibration. However, tilting the C–O axis about its center of mass by 10° away from its average orientation changes θ_{eq} by less than one degree. Hence, neglect of H_2CO vibrations is justified. Finally, it has been assumed throughout this paper that the HF bond length is unchanged from the free molecule value. This assumption affects the values of the angular expectation values derived from the HF hyperfine constants, and hence its effect on the modeling of the equilibrium structure must be probed. It is found that a lengthening of the HF bond in the complex does not change the determined equilibrium angle, but lowers the value obtained for the amplitude. In particular, if the HF bond lengthens by the reasonable amount of 0.01 Å on complex formation, θ_{eq} is found to be 23.8° and α becomes 15.5°. The harmonic vibrational frequency associated with this amplitude is close to the value obtained by infrared spectroscopy in the matrix isolation study.

The result obtained through use of this simple model is consistent with the measured dipole moment components of the complex. Using the known values for the submolecule dipole moments, the expressions for the average values of the direction cosines of the HF axis in terms of θ_{eq} and α, and the average orientation of the CO axis determined from the rotational constants, the dipole moment projections along the a and b axes are found to be 2.894 and 1.232 D, respectively, where the sign of the b component is determined by the sign of the H_2CO dipole moment. The dipole moment enhancements thus obtained are 0.86 and 0.17 D for the a and b components, respectively. If, however, HF is assumed to point at the oxygen atom in the equilibrium configuration, the direction cosines appropriate to the HF axis change resulting in a decrease in the b-axis projection of the HF dipole moment. The calculated b-axis projection of the total dipole moment hence becomes larger than the observed value (the calculated b component is 1.542 D for this case). The negative dipole moment enhancement implied by this is totally unexpected from considerations of the polarizabilities of HF and H_2CO.[33]

In conclusion, a molecular beam study of the prototypical hydrogen bonded complex H_2CO–HF has been carried out. High resolution microwave and radio-frequency spectroscopy has yielded precision rotational constants, dipole moment components, and HF hyperfine constants for the isolated complex. The average orientation in the complex of the heavy atoms is well determined by the rotational constants. The HF axis orientation is well defined by the HF direct nuclear spin–spin coupling tensor. The observation of hyperfine splittings attributable to the presence of the triplet spin state of formaldehyde provides information regarding the possibility of tunneling between the two equivalent forms of H_2CO–HF that shows the molecule to be fairly rigid. Finally, measured hyperfine constants and dipole moment components of the complex are best accounted for by an equilibrium structure in which the hydrogen bond is allowed to deviate ~9° from a linear arrangement.

ACKNOWLEDGMENTS

The expert advice of Dr. Stephen L. Coy on klystron synchronization techniques as well as the loan of equipment from Dr. Coy and Professor Harry Radford is gratefully acknowledged.

[1]T. H. Lowry and K. S. Richardson, *Mechanism and Theory in Organic Chemistry* (Harper & Row, New York, 1976), pp. 405–416.
[2]I. Olovsson and P.-G. Jönsson, *The Hydrogen Bond—Recent Developments in Theory and Experiments*, edited by P. Schuster, G. Zundel, and C. Sandorfy (North–Holland, Amsterdam, 1976).
[3](a) *The Hydrogen Bond—Recent Developments in Theory and Experiments*, edited by P. Schuster, G. Zundel, and C. Sandorfy (North–Holland, Amsterdam, 1976), Chaps. 12 and 16. (b) G. C. Pimentel and A. L. McClellan, *The Hydrogen Bond* (Freeman, San Francisco, 1960), Chap. 3.
[4](a) B. Nelander, J. Mol. Struct. **69**, 59 (1980); (b) Reference 3(a), Chap. 22.
[5]R. F. W. Bader, I. Keaveny, and P. E. Cade, J. Chem. Phys. **47**, 3381 (1967).
[6]M. K. Orloff and N. B. Colthup, J. Chem. Ed. **50**, 401 (1973).
[7]J. A. Shea and W. H. Flygare, J. Chem. Phys. **76**, 4857 (1982).
[8]P. D. Aldrich, A. C. Legon, and W. H. Flygare, J. Chem. Phys. **75**, 2126 (1981).
[9]M. S. Gordon, D. E. Tallman, C. Monroe, M. Steinbach, and J. Armburst, J. Am. Chem. Soc. **97**, 1326 (1975).
[10]A. S. N. Murthy, G. R. Saini, K. Devi, and S. B. Shah, Adv. Mol. Relaxation Processes **7**, 255 (1975).
[11]J. E. DelBene, Chem. Phys. Lett. **24**, 203 (1974).
[12]J. Sadlej, Rocz. Chem. **51**, 1013 (1977).
[13]K. Romanowska and H. Ratajczak, Teor. Eksp. Khim. **13**, 521 (1977).
[14]M. Tsuda, H. Touhara, K. Nakanishi, and N. Watanabe, Bull. Chem. Soc. Jpn. **49**, 2391 (1976).
[15]P. A. Kollman, J. McKelvey, A. Johansson, and S. Rothenberg, J. Am. Chem. Soc. **97**, 955 (1975).
[16]P. Schuster, Theor. Chim. Acta **19**, 212 (1970).
[17]F. S. Dainton, K. J. Ivin, and D. A. G. Walmsley, Trans. Faraday Soc. **55**, 61 (1959).
[18]T. C. English and J. C. Zorn, *Methods of Experimental Physics*, 2nd ed., edited by D. Williams (Academic, New York, 1972), Vol. 3.
[19]C. S. Townes and A. L. Schawlow, *Microwave Spectroscopy* (McGraw-Hill, New York, 1955), Chap. 4.
[20]W. Gordy and R. L. Cook, *Microwave Molecular Spectra*, Part II of *Chemical Applications of Spectroscopy*, 2nd. ed., edited by W. West (Wiley–Interscience, New York, 1970).
[21]J. K. G. Watson, J. Chem. Phys. **46**, 1935 (1967).
[22]P. Thaddeus, L. C. Krisher, and J. H. N. Loubser, J. Chem. Phys. **40**, 257 (1964).
[23]T. A. Dixon, C. H. Joyner, F. A. Baiocchi, and W. Klem-

perer, J. Chem. Phys. **74**, 6539 (1981).
[24]The sign of the HF dipole moment is $^+HF^-$. The sign of the H_2CO dipole moment is $^+CO^-$.
[25]The b-axis projection of the H_2CO dipole moment is 1.94 D, a value greater than the observed μ_b of H_2COHF.
[26]J. R. de la Vega, Acc. Chem. Res. **15**, 185 (1982); E. Merzbacher, *Quantum Mechanics*, 2nd ed. (Wiley, New York, 1970), pp. 65–78.
[27]R. Viswanathan and T. R. Dyke, J. Chem. Phys. **77**, 1166 (1982).
[28]P. H. Turner, A. P. Cox and J. A. Hardy, J. Chem. Soc. Faraday Trans 2 **77**, 1217 (1981).
[29]E. B. Wilson, Jr., J. C. Decius, and P. C. Cross, *Molecular Vibrations* (Dover, New York, 1980), Appendix III.
[30]P. A. Kollman, J. Am. Chem. Soc. **94**, 1837 (1972).
[31]P.-G. Jönsson, Acta Crystallogr. Sect. B **27**, 893 (1971).
[32]Lester Andrews (private communication).
[33]The polarizability of H_2CO is greater than that of HF. Since the sign of the b component is determined by the H_2CO dipole moment, induction effects will increase the value calculated from simple projection. The polarizability of HF is found in J. S. Muenter, J. Chem. Phys. **56**, 5409 (1972); that of H_2CO is found in J. Applequist, J. R. Carl, and K. K.-K. Fung, J. Am. Chem. Soc. **94**, 2952 (1972).